

Computation of Turbulent Flow Through Parallel Plates with Streamwise Periodic Ribs by a Method with Self-adjusted Relaxation Factor

Wen-Bin Tsai

Department of Management Information System, Far East College
No. 49, Chung-Hua Road,,Hsin-Shih, Tainan County 744, Taiwan.
wbtsai@cc.fec.edu.tw
TEL : 886-6-5977601, FAX : 886-6-5977600

ABSTRACT

In this study, the flow-field and forced-convection characteristics of turbulent flow through plates with streamwise periodic ribs is simulated by a faster converged numerical method. The method based on self-adjusted under relaxation factors is motivated from the concept of Bi-CGSTAB algorithm, which updates the solution vectors by the 2-norm minimization of the residual vectors of the governing equations, thus the optimal selection of the under relaxation factors for each control volume can be determined and hence the faster convergence for the numerical simulation can be achieved. In the flow-field, the upper wall is assumed thermally insulated, whereas the bottom plate with streamwise rectangular periodic ribs is provided with a uniform heat flux. The flow field and heat transfer characteristics are predict by Durbin's $k-\varepsilon-v^2$ model, the numerical approach is based on the finite volume technique with staggered grid arrangement, and the PISO algorithm is adopted to obtain the pressure and the velocities. The local Nusselt number distribution along the bottom wall is calculated and compared with the experiment results concluded by Lorenz, et al. It also compared with the computed results of Luo et al. The proposed method adopts the self-adjusted under relaxation factor provides the accurate flow-field and the forced-convection characteristics, furthermore, it indeed accelerates the convergence in this numerical simulation.

Keywords : relaxation factors , Bi-CGSTAB, Nusselt number, faster convergence

1. Introduction

Repeated rib-turbulators created in flow passage at periodic intervals can enhance the removal of heat transfer. The flow separation zones ahead and after the ribs increase the turbulence and heat transfer levels significantly. It is of practical importance and employed in blade and other cooling applications. In this paper, numerical computations on the flow-field and heat transfer characteristics in a rectangular channel with streamwise-periodic ribs mounted on one of the principal walls are performed based on the heat transfer measurements by Lorenz et al.[1], The numerical prediction was also compared to the results of Luo et al. [2], which are computed by standard $k-\varepsilon$ model and RSM model. Furthermore, a numerical method motivated from the Bi-CGSTAB algorithm with self-adjusted under relaxation factor is applied to enforce the faster convergence.

2. Governing Equations

Turbulent flow are commonly encountered in practical applications, thus the time-mean behavior of these flows are usually of practical interest. Therefore, the equations for unsteady laminar flow are converted into the time-averaged equations for turbulent flow by an averaging operation in which it is assumed that there are rapid and random fluctuation about the mean value. In our study, the time dependent, Reynolds averaged, incompressible Navier-Stokes equations and transport equations of turbulent properties are solved to obtain the turbulent flow-field and temperature field.

In this study, an incompressible fully developed turbulent flow was chosen as the flow pass through a channel, the upper wall is assumed thermally insulated, whereas the bottom plate with streamwise rectangular periodic ribs is provided with a uniform heat flux. The concepts of fully developed flow and heat transfer have

been generalized to accommodate ducts whose cross-sectional area varies periodically in the streamwise direction. The identification of the periodicity characteristics of the velocity components and of a reduced pressure functions enable the flow field analysis to be confined to a single isolated module, without involvement with the entrance region problem. Patankar [3] formulate a generalization of the concept of the fully developed flow and heat transfer to accommodate ducts of periodically varying cross section, which enable the fully developed solution to be obtained for these duct flows without having to deal with the entrance region. The governing equations can be reduced to the following form by Patankar's formulation, e.g.

Continuity Equation :

$$\frac{\partial U_i}{\partial x_j} = 0 \quad (1)$$

Momentum Equations :

$$\frac{\partial(\rho U_i)}{\partial t} + \frac{\partial(\rho U_i U_j)}{\partial x_j} = -\frac{\partial \hat{P}}{\partial x_j} + \frac{\partial}{\partial x_j} \left[\mu \left(\frac{\partial U_i}{\partial x_j} + \frac{\partial U_j}{\partial x_i} \right) - \overline{\rho u_i u_j} \right] \quad (2)$$

In the fully developed region, the pressure drop per pitch is a constant (β), i.e. $P(x + Pi, y) = P(x, y) - \beta \cdot Pi$, Pi is the pitch length. Thus, if we use the notation $\hat{P}(x, y) = \beta x + P(x, y)$, then we have the following relation:

$$\hat{P}(x + n \cdot Pi, y) = \hat{P}(x + (n-1) \cdot Pi, y) = \dots = \hat{P}(x, y) \quad (3)$$

where n is an integer and \hat{P} repeats itself from pitch to pitch.

Energy Equations :

$$\frac{\partial(\rho \hat{T})}{\partial t} + \frac{\partial(\rho U_i \hat{T})}{\partial x_i} = \frac{\partial}{\partial x_i} \left[\left(\frac{\mu}{Pr} + \frac{\mu_t}{Pr_t} \right) \frac{\partial \hat{T}}{\partial x_i} \right] - \rho U_i \gamma \delta_{ii} \quad (4)$$

where Pr is the Prandtl number, Pr_t is the turbulent Prandtl number, δ_{ii} is the Kronecker delta function, l is the streamwise direction, $\hat{T} = T - \gamma x$, and γ is the temperature gradient across one pitch which is defined as $\gamma = \frac{T(x + Pi, y) - T(x, y)}{Pi}$.

3. Durbin's $k - \varepsilon - v^2$ model [4]

$$\frac{\partial(\rho k)}{\partial t} + \frac{\partial(\rho U_j k)}{\partial x_j} = \frac{\partial}{\partial x_j} \left[\left(\mu + \frac{\mu_t}{\sigma_k} \right) \frac{\partial k}{\partial x_j} \right] + P_k - \rho \varepsilon \quad (5)$$

$$\frac{\partial(\rho \varepsilon)}{\partial t} + \frac{\partial(\rho U_j \varepsilon)}{\partial x_j} = \frac{\partial}{\partial x_j} \left[\left(\mu + \frac{\mu_t}{\sigma_\varepsilon} \right) \frac{\partial \varepsilon}{\partial x_j} \right] + \frac{\rho C_{\varepsilon 1} P_k - \rho C_{\varepsilon 2} \varepsilon}{T} \quad (6)$$

$$\frac{\partial(\rho \overline{v^2})}{\partial t} + \frac{\partial(\rho U_j \overline{v^2})}{\partial x_j} = \frac{\partial}{\partial x_j} \left[\left(\mu + \frac{\mu_t}{\sigma_k} \right) \frac{\partial \overline{v^2}}{\partial x_j} \right] + \rho k f - \rho \overline{v^2} \frac{\varepsilon}{k} \quad (7)$$

$$L^2 \nabla^2 f - f = (1 - C_1) \frac{\left[\frac{2}{3} \frac{\overline{v^2}}{k} \right]}{T} - C_2 \frac{P_k}{k}, \quad (8)$$

$$\mu_t = \rho C_\mu \overline{v^2} T. \quad (9)$$

where $\sigma_k = 1.0$, $\sigma_\varepsilon = 1.3$, $C_{\varepsilon 1} = 1.3 + \frac{0.25}{1 + \left(\frac{d}{2\ell}\right)^8}$, $C_{\varepsilon 2} = 1.9$, $C_\mu = 0.19$, $C_L = 0.3$, $C_\eta = 70$, $\ell = \frac{L}{C_L}$,

$C_1 = 1.4$, $C_2 = 0.3$, d : distance to the closest boundary, $L = C_L \max\left(\frac{k^{1.5}}{\varepsilon}, C_\eta \left(\frac{\nu^3}{\varepsilon}\right)^{\frac{1}{4}}\right)$, $T = \max\left(\frac{k}{\varepsilon}, 6\left(\frac{\nu}{\varepsilon}\right)^{\frac{1}{2}}\right)$.

Durbin's $k - \varepsilon - v^2$ model is proposed for computing non-equilibrium, or complex, turbulent flows. In his model, the velocity scale for turbulent transport toward the wall is $\overline{v^2}$, not k . Extra two parameters $\overline{v^2}$ and f , need to be solved via $\overline{v^2}$ transport equation and an elliptic relaxation equations for f . The variable $\overline{v^2}$ is a velocity

scale and might loosely be regarded as the velocity fluctuation normal to the streamlines. Also, $\overline{v^2}$ behaves as the wall normal component of turbulent intensity near the surfaces. Impermeable boundaries cause non-local suppression of $\overline{v^2}$, and the elliptic relaxation equation for f is the mathematical representation of non-locality. It is designed to use in wall-bounded flows. Good agreement between experiment and predictions are obtained for turbulent channel flow [5], turbulent separated flows over a backward facing step [4], in a plane diffuser, and around a triangular cylinder, jet impinging onto a pedestal [6], and applied to transonic flows. Furthermore, a potential advantage of the $k - \varepsilon - v^2$ model over the $k - \varepsilon$ model is that $\overline{v^2}/k$ provides a measure of anisotropy. Of course, the crucial role of anisotropy near walls was the original motivation for $k - \varepsilon - v^2$ model: the $\overline{v^2}$ - equation enables the model to be integrated to the wall without damping functions because it acknowledges this important property of the turbulence.

4. Numerical Procedure

In order to discretize the governing equations, finite volume approach with staggered grid arrangements are employed. According to expressions of Patankar [7], the difference equations for every control volume can be expressed in the following form

$$\left[a_p^* + \frac{\rho \text{vol}}{\Delta t} \right] \phi_p^{k+1} = \sum a_{nb} \phi_{nb}^{k+1} + c_p^* + \frac{\rho \text{vol}}{\Delta t} \phi_p^k + S_p \phi_p^{k+1} + S_u \quad (10)$$

where a_{nb} represents the positive coefficients a_E, a_W, a_N, a_S , which are obtained by hybrid scheme for convective terms and central difference scheme for diffusion terms, a_p^* is the sum of these neighbor coefficients, i.e. $a_p^* = a_E + a_W + a_N + a_S$; vol represents the volume of the cell-P, Δt is the time stepsize at cell-P, ρ is the density and S_u and S_p are the source terms ($S_p \leq 0$). Therefore, the equations can be casted into

$$\left[a_p + \frac{\rho \text{vol}}{\Delta t} \right] \phi_p^{k+1} = \sum a_{nb} \phi_{nb}^{k+1} + c_p + \frac{\rho \text{vol}}{\Delta t} \phi_p^k \quad (11)$$

where $a_p = a_p^* - S_p, c_p = c_p^* + S_u$. By the application of under-relaxation factors, the above difference equations can also be represented as

$$\frac{1}{\alpha_p} a_p \phi_p^{k+1} = \sum a_{nb} \phi_{nb}^{k+1} + c_p + \frac{1 - \alpha_p}{\alpha_p} \phi_p^k \quad (12)$$

where $0 < \alpha_p \leq 1$ is the under-relaxation factor for cell-P. Furthermore, the above difference equations can be combined to the following matrix form at the k-th time step,

$$(A_k + D_{k+1}) \phi_{k+1} = b_k + D_{k+1} \phi_k \quad (13)$$

where the vectors ϕ_k, ϕ_{k+1} represent the solutions for the k-th and (k+1)-th time step respectively, the coefficient matrix A_k is a penta-diagonal M -matrix, and D_{k+1} is a positive diagonal matrix relating the under relaxation factor, i.e. D_{k+1} is a positive diagonal matrix and the j-th diagonal element is

$$\text{diag}(D_{k+1})_j = \frac{1 - \alpha_j}{\alpha_j} (a_p)_j \quad (14)$$

where α_j is the under relaxation factor for the j-th control volume.. Traditionally, the under relaxation factor α_j is set to be a constant, here, we supposes that α_j is different for each control volume and is determined from the Bi-CGSTAB method due to the residual minimization. [8, 9].

5. Determination of Under Relaxation Factors

It is well known that the small under relaxation factors will cause slow convergence but large under relaxation factors will lead to divergence or oscillation for the numerical simulation. A suggestion on the optimal choice of the under relaxation factors is thus of interest. The governing equations are transformed to difference equations as a linear system of eq. (15) before the numerical procedure.

$$(A_k + D_{k+1})\phi_{k+1} = b_k + D_{k+1}\phi_k \quad (15)$$

In eq. (15), the coefficient matrix A_k and the vector b_k in the right hand side are computed from the k-th time step solutions. Matrix D_{k+1} is a diagonal matrix and its elements are evaluated at (k+1)-th step. The residual vector for the k-th time step is defined by

$$r_k = b_k - A_k\phi_k + D_k(\phi_{k-1} - \phi_k) \quad (16)$$

Comparing to existing iterative algorithms solving the matrix system, an additional parameter as adjustable under relaxation factors from the analogy of the Bi-CGSTAB algorithm is derived and described as follows. Table 1 lists two solution procedures of two iterative algorithms to solve the linear systems $Ax = b$ and $(A_k + D_{k+1})\phi_{k+1} = b_k + D_{k+1}\phi_k$, which conveys the idea determining the under relaxation factors. Algorithm I in Table1 lists the solution procedure for the standard Bi-CGSTAB algorithm while solving a linear system of the form. The initial residual $r_0 = b - Ax_0$ is defined from the initial guess x_0 . According to the algorithm, the next solution vector and residual vector are $x_1 = x_0 + \alpha p_1 + \omega_1 s$ and $r_1 = s - \omega_1 t$ respectively, and the parameter ω_1 is derived from the minimization of the vector r_1 . Hence, the solution vector is updated under the restriction of the 2-norm minimization of the corresponding residual vector. Consequently, the (i+1)-th approximation solution x_{i+1} is updated by the relation $x_{i+1} = x_i + \alpha p_i + \omega_{i+1} s$, where the parameter ω_{i+1} is determined such that the norm $\|r_{i+1}\|_2 = \|s - \omega_{i+1} t\|_2$ a minimal value.

The concept of minimizing residual is extended to time span in the computation of turbulent flow, such that the chosen under relaxation factors will enforce the residual to a minimum value in next time step. Algorithm II in Table 1 is designed to determine the under relaxation factors for solving the linear system (15) in each time step, where D_{k+1} involves the under relaxation factors but A_k involves no under relaxation factors. In algorithm II, the coefficient matrix A_0 and the vector b_0 are obtained from the initial guess value x_0 , and the residual vector thus can be defined as $r_0 = b_0 - A_0 x_0$. Moreover, A_k, x_k, r_k are the coefficient matrix, solution vector and residual vector at the k-th time step respectively and the linear system

$$(A_k + D_{k+1})x_{k+1} = b_k + D_{k+1}x_k \quad (17)$$

are solved at the (k+1)-th time step. Similar to the procedure in algorithm I in Table 1, the solution vector x_{k+1} for the (k+1)-th time step follows both $x_{k+1} = x_k + \alpha p_{k+1} + \omega_{k+1} s$ and D_{k+1} needs to be determined such that the system eq. (17) can be solved.

Since the residual vectors are defined by

$$r_k = b_k - A_k x_k + D_k(x_{k-1} - x_k) \quad (18)$$

and x_k is updated to x_{k+1} by

$$x_{k+1} = x_k + \alpha p_{k+1} + \omega_{k+1} s \quad (19)$$

Subtracting Eq. (17) by $(A_k + D_{k+1})x_k$ on both sides of equal sign, Eq. (17) yields to

$$(A_k + D_{k+1})(x_{k+1} - x_k) = b_k + D_{k+1}x_k - (A_k + D_{k+1})x_k = b_k - A_k x_k \quad (20)$$

Substituting equation Eq. (18) to Eq. (20), we have

$$(A_k + D_{k+1})(x_{k+1} - x_k) = r_k - D_k(x_{k-1} - x_k) \quad (21)$$

Combining Eq. (19) and Eq. (21) we can determine D_{k+1} by the following relation

$$(A_k + D_{k+1})(\alpha p_{k+1} + \omega_{k+1} s) = r_k - D_k(x_{k-1} - x_k) \quad (22)$$

or the following relation

$$D_{k+1}(\alpha p_{k+1} + \omega_{k+1} s) = r_k - D_k(x_{k-1} - x_k) - A_k(\alpha p_{k+1} + \omega_{k+1} s) \quad (23)$$

Note that D_{k+1} is a positive diagonal matrix, thus the under relaxation factors for the j-th control volume can be determined. That is, the under relaxation factors for each control volume at different instant of time is different, which is completely different from the conventional methods.

Table 1 : Comparison of conventional iterative Bi-CGSTAB algorithm (Algorithm I) with the proposed solution procedure (Algorithm II)

Algorithm I : Solve $Ax = b$	Algorithm II : Solve $(A_k + D_{k+1})x_{k+1} = b_k + D_{k+1}x_k$
Give x_0 and $r_0 = b - Ax_0$ Choose $\hat{r}_0 = r_0$ $\rho_0 = \alpha = \omega_0 = 1, v_0 = p_0 = 0$ For $i=1,2,3,\dots$ $\rho_i = (\hat{r}_0, r_{i-1})$ $\beta = \frac{\rho_i}{\rho_{i-1}} \frac{\alpha}{\omega_{i-1}}$ $p_i = r_{i-1} + \beta(p_{i-1} - \omega_{i-1}v_{i-1})$ $v_i = Ap_i$ $\alpha = \frac{\rho_i}{(\hat{r}_0, v_i)}$ $s = r_{i-1} - \alpha v_i$ $t = As$ $\omega_i = \frac{(t, s)}{(t, t)}$ $x_i = x_{i-1} + \alpha p_i + \omega_i s$ If x_i is accurate enough then stop $r_i = s - \omega_i t$ $i=i+1$ endfor	Give x_0 and $r_0 = b_0 - A_0 x_0$ Choose $\hat{r}_0 = r_0$ $\rho_0 = \alpha = \omega_0 = 1, v_0 = p_0 = 0$ For $k=0,1,2,\dots$ $\rho_{k+1} = (\hat{r}_0, r_k)$ $\beta = \frac{\rho_{k+1}}{\rho_k} \frac{\alpha}{\omega_k}$ $p_{k+1} = r_k + \beta(p_k - \omega_k v_k)$ $v_{k+1} = (A_k + D_k)p_{k+1}$ $\alpha = \frac{\rho_{k+1}}{(\hat{r}_0, v_{k+1})}$ $s = r_k - \alpha v_{k+1}$ $t = (A_k + D_k)s$ $\omega_{k+1} = \frac{(t, s)}{(t, t)}$ Determine D_{k+1} from $(A_k + D_{k+1})^{-1} [res - x^k + D_k(x_k - x_{k-1})]$ $= \alpha p_{k+1} + \omega_{k+1} s$ Solve x_{k+1} from $(A_k + D_{k+1})x_{k+1} = b_k + D_{k+1}x_k$ If x_i is accurate enough then stop Compute A_{k+1}, b_{k+1} Compute $res - x^{k+1} = r_{k+1}$ $= b_{k+1} - A_{k+1}x_{k+1} + D_{k+1}(x_k - x_{k+1})$ $k=k+1$ endfor

6. Results and Discussions

The Reynolds number based on the channel hydraulic diameter of the computed fluid flow is 9.4×10^4 . For the computational geometry in figure 1, the width-to-height ratio of the rib was 2 (e.g. $w/h=2$), the pitch-to-height ratio was 4 (e.g. $L/h=4$), the height-to-hydraulic-diameter ratio was 4 (e.g. $(H-h)/h=4$ or $H/h=3$). As the passage is long enough for repeating flow conditions to prevail over each rib interval, the numerical flow domain cover only one rib interval and periodic flow boundary conditions are applied. The result predicted here are obtained using 134×178 grid system.

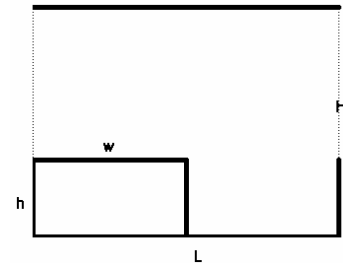


Figure 1 : Computational geometry

Figure 2 shows the convergence histories of velocities for turbulent flow past a surface mounted rib. In this picture, the influence of different choice of under relaxation factors is compared, the chosen of a larger number of under relaxation factor α_{max} leads to divergence, the chosen of a smaller value of under relaxation factor $\alpha_{min}=0.7$ leads to a slower convergence, After many tests runs, the constant time step of $\alpha = 0.91$ gives us the fastest convergence rate if the under relaxation factor is constant. The convergence behavior for the chosen

of self-adjusted under relaxation factors and the results by $\alpha_{const}=0.91$ are similar, but the convergence rate for the proposed method is faster than the other chosen of constant relaxation factors.

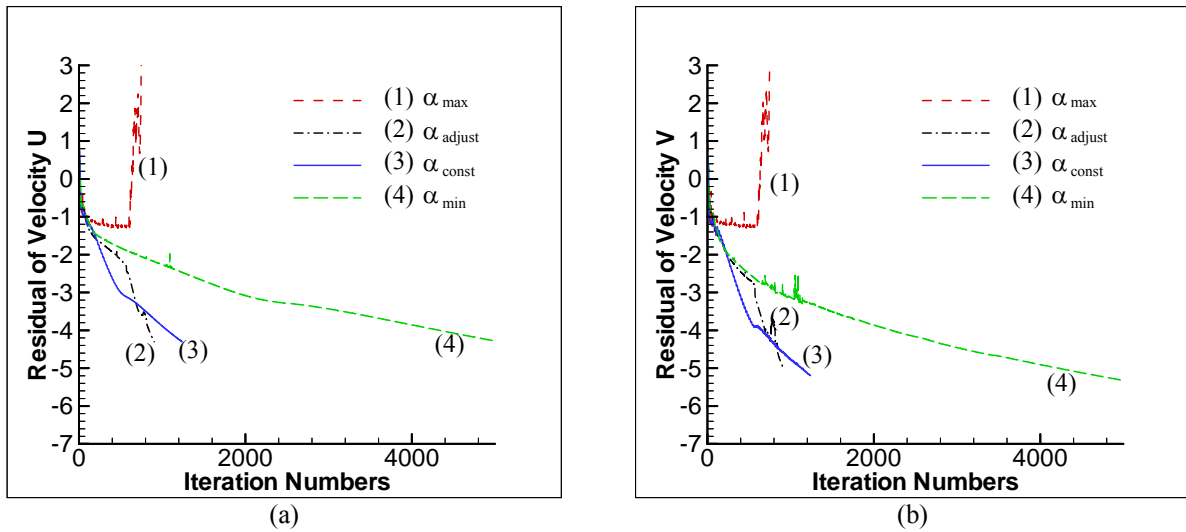


Figure 2 : Residual histories of different variables (by Durbin's model): (a) velocity U (b) Velocity V

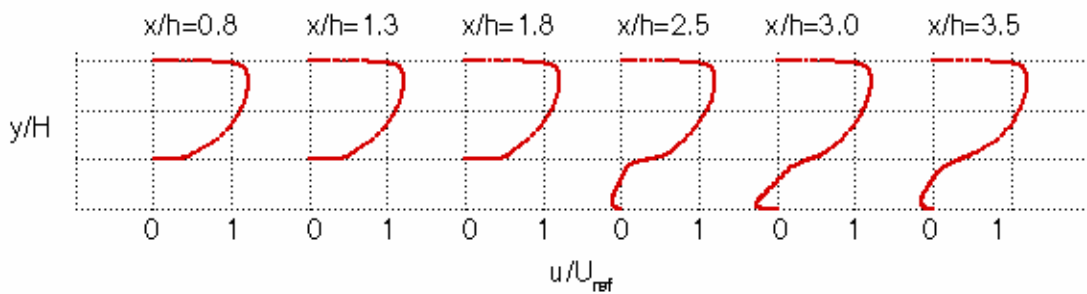


Figure 3 : Streamwise velocity profiles for different locations

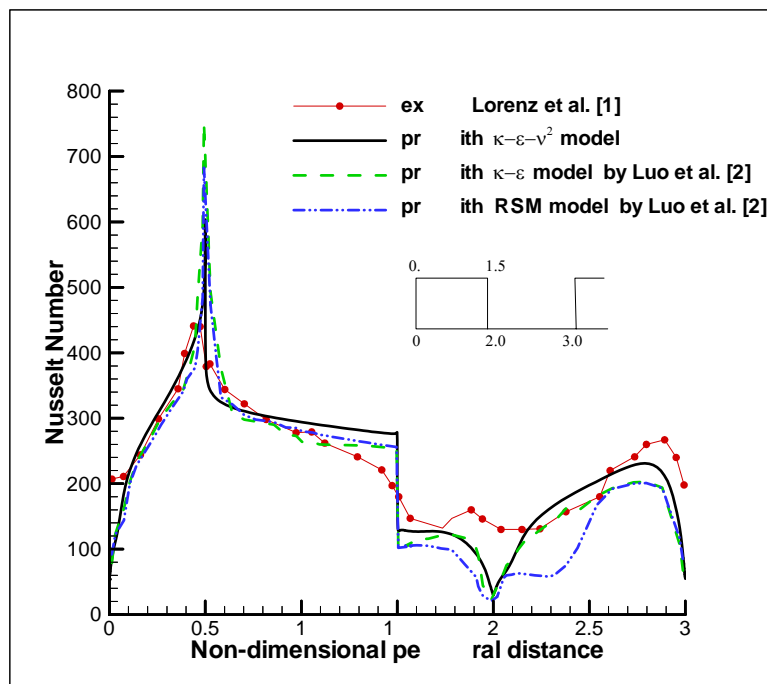


Figure 3 : Nusselt number distribution ($R_{ed} = 94,000$)

Figure 3 shows the streamwise velocity profiles for different locations downstream the flow passage, For $x/h=0.8, 1.3$ or 1.8 , the locations are above the rib, hence no recirculation zone is found. However, for locations $x/h=2.5, 3.0$ or 3.5 , the computations obtain the main feature of the flow field with somewhat different sizes of separation bubbles ahead of the rib. The computed local Nusselt number is compared with the experiment of Lorenz et al. [1] and the computed results by Luo et al [2]. Figure 4 presents the measured and computed Nusselt number distribution by various turbulence models. It is interested to note that, the computed heat transfer coefficient fits well with measured distribution for these three models. However, Durbin's model provides better prediction for the bottom wall at $s=2.0$ to 3.0 . The proposed method with self-adjusted under relaxation factor not only provides the faster convergence rate, but also provides the accurate forced-convection characteristics (local Nusselt number distribution) along the bottom wall.

7. Conclusions

The proposed method motivated from the Bi-CGSTAB algorithm adopted the self-adjusted under relaxation factor technique, and the Durbin's higher accurate $k - \epsilon - v^2$ turbulence model is applied to simulate the flow-field and forced-convection characteristics of turbulent flow through plates with streamwise periodic ribs. The numerical results indicated that, not only the proposed method is a faster converged numerical method but also provides the accurate forced-convection characteristics (local Nusselt number distribution) along the heated bottom wall.

7. Acknowledgement

The author want to thank the National Science Council, Taiwan, for the fully support of this research work under Contract NSC-94-2115-M-269-001.

8. References

- [1] S. Lorenz, D. Mukomilow, and W. Leiner: *Distribution of heat transfer coefficients in a channel with periodic transverse Grooves*. Experimental Thermal and Fluid Science, 11: 234-242, 1995.
- [2] D. D. Luo, C. W. Leung, T. L. Chan, and W. O. Wong, *Flow and forced convection characteristics of turbulent flow through parallel plates with periodic transverse ribs*. Numerical Heat Transfer, Part A, 48: 43-48, 2005.
- [3] S. V. Patankar, C.H. Liu and E. M. Sparrow, *Fully Developed Flow and Heat Transfer in Ducts Having Streamwise-Periodic Variations of Cross-sectional Area*, Transaction of the ASME, Journal of Heat Transfer, vol. 99, May, pp. 180-186, 1977.
- [4] P. A. Durbin, *Separated Flow Computations with the $k - \epsilon - v^2$ Mode*", AIAA Journal, vol. 33, No. 4, April, pp. 659-664, 1995.
- [5] P. A. Durbin, *Near-Wall Turbulence closure Modeling Without Damping Functions*, Theoret. Comput. Fluid Dynamics, vol. 3, pp. 1-13, 1991.
- [6] P. A. Durbin, Y. Shabany, S. Parneix and M. Behnia, *Connections of Lagrangian Dissipation Theory to Heat Transfe*", 2nd Int. Symposium on Turbulence, Heat and Mass Transfer, Delft, The Netherlands, June, pp. 47-54, 1997.
- [7] S. V. Patankar, *Numerical Heat Transfer and Fluid Flow*, Hemisphere Publishing Corporation, Washington, New York, Londo, 1980.
- [8] W. B. Tsai, W. W. Lin and C. C. Chieng, "Convergence Acceleration by Varying Time-Step Size Using Bi-CGSTAB Method for Turbulent Flow Computation", *Numerical Methods for Partial Differential Equations*, **17**, 454-474, 2001.
- [9] W. B. Tsai, W. W. Lin and C. C. Chieng, "Convergence Acceleration by Self-Adjusted Time Stepsize Using Bi-CGSTAB Method for Separated Flow Computation", *International Journal for Numerical Methods in Fluids*, **39**, 141-159, 2002.
- [10] W. B. Tsai, C. J. Hsieh, and C. C. Chieng, *Parallel computation of electroosmotic flow in L-shaped microchannels*: 6th World Congress of Structural and Multidisciplinary Optimization, Rio de Janeiro, 2005.